Effect of Distortions in the Deoxyribose Phosphate Backbone Conformation of Duplex Oligodeoxyribonucleotide Dodecamers Containing GT, GG, GA, AC, and GU Base-Pair Mismatches on ^{31}P NMR Spectra†

Vikram A. Roongta, Claude R. Jones, and David G. Gorenstein*
Department of Chemistry, Purdue University, West Lafayette, Indiana 47907
Received December 12, 1989; Revised Manuscript Received February 2, 1990

ABSTRACT: We have previously suggested that variations in the ^{31}P chemical shifts of individual phosphates in duplex oligonucleotides are attributable to torsional angle changes in the deoxyribose phosphate backbone. This hypothesis is now directly supported by analysis of the $^{1}H/^{31}P$ two-dimensional *J*-resolved spectra of a number of mismatch dodecamer oligonucleotide duplexes including the following sequences: d-(CGTGAATTCGCG), d(CGUGAATTCGCG), d(CGGGAATTCGCG), d(CGAGAATTCGCG), and d(CGCGAATTCACG). The ^{31}P NMR signals of the dodecamer mismatch duplexes were assigned by 2D $^{1}H/^{31}P$ *p*ure *a*bsorption phase *c*onstant time (PAC) heteronuclear correlation spectra. From the assigned H3′ and H4′ signals, the ^{31}P signals of the base-pair mismatch dodecamers were identified. $J_{H3'-P}$ coupling constants for each of the phosphates of the dodecamers were obtained from $^{1}H/^{31}P$ *J*-resolved selective proton flip 2D spectra. By use of a modified Karplus relationship, the C4′–C3′–O3′–P torsional angles (ϵ) were obtained. $J_{H3'-P}$ coupling constants were measured for many of the oligonucleotides as a function of temperature. There exists a good linear correlation between ^{31}P chemical shifts and the ϵ torsional angle. This correlation can be further extended to the C3′–O3′–P–O5′ torsional angle (ζ) by using a linear relationship between ϵ and ζ obtained from crystal structure studies. The ^{31}P chemical shifts follow the general observation that the more internally the phosphate is located within the oligonucleotide sequence, the more upfield the ^{31}P resonance occurs. In addition, ^{31}P chemical shifts show sequence- and site-specific variations. Analysis of the backbone torsional angle variations from the coupling constant analysis has provided additional information regarding the origin of these variations in ^{31}P chemical shifts.

It is now widely appreciated that duplex DNA can exist in a number of different conformations (Saenger, 1984). Significant conformational differences can exist globally along the entire double helix, as in the A-, B-, C-, and Z-forms of DNA (Saenger, 1984). In addition, local conformational heterogeneity in the deoxyribose phosphate backbone has been most recently noted in the form of sequence-specific variations (Calladine, 1982; Dickerson, 1983; Dickerson & Drew, 1981) or as the result of drug (Saenger, 1984) or protein binding (Hochschild & Ptashne, 1986; Martin & Schleif, 1986; McClarin et al., 1986) to local regions of the DNA. While X-ray crystallography has provided much of our understanding of these DNA structural variations, increasingly, high-resolution NMR (particularly $^{1}H/^{1}H$ NOESY) has also begun to provide detailed three-dimensional structural information on duplex oligonucleotides (Broido et al., 1984; Feigon et al., 1983; Frechet et al., 1983; Hare et al., 1983; James, 1984; Kearns, 1984; Scheek et al., 1984; Schroeder et al., 1986, 1987; van de Ven & Hilbers, 1988). Importantly, NMR experiments have suggested that the duplex conformation in solution (Assa-Munt & Kearns, 1984; Clore et al., 1985; Gorenstein et al., 1988; Nikonowicz et al., 1989; Patel et al., 1987; Rinkel et al., 1987) may not be identical with the static picture provided by X-ray diffraction in the crystal state. This has raised the question whether some of the sequence-specific structural variations observed in the X-ray crystallographic studies are the result of less profound crystal packing forces.

In addition, while base pairing and stacking interactions can often be adequately defined from NOESY-derived distances (Nilges et al., 1987), detailed sequence-specific conformational information with regard to the deoxyribose phosphate backbone is often not available (van de Ven & Hilbers, 1988). Recently we have attempted to utilize ^{31}P NMR to define sequence-specific variations in the *backbone* conformation of oligonucleotides (Gorenstein et al., 1988; Nikonowicz et al., 1989; Schroeder et al., 1989). Variations of ^{31}P chemical shifts of individual phosphates in duplex oligonucleotides have been suggested to be attributable to torsional angle changes in the deoxyribose phosphate backbone. This hypothesis is now directly supported by analysis of the $^{1}H/^{31}P$ two-dimensional *J*-resolved spectra of the dodecamer mismatch duplexes d-(CGTGAATTCGCG), d(CGUGAATTCGCG), d-(CGGGAATTCGCG), d(CGAGAATTCGCG), and d-(CGCGAATTCACG) as well as a number of 10-, 12-, 13-, and 14-mers from our laboratory.

Stereoelectronic Effect on ^{31}P Chemical Shifts as a Probe of DNA Structure. Our laboratory has suggested that ^{31}P chemical shifts can potentially provide a probe of the conformation of the phosphate ester backbone in nucleic acids and nucleic acid complexes (Gorenstein, 1978, 1981, 1984; Gorenstein et al., 1987a,b). Molecular orbital calculations in our laboratory provided initial suggestions that ^{31}P chemical shifts were influenced by conformation-dependent orbital interactions, which we have ascribed to a stereoelectronic effect (Gorenstein, 1987). These calculations (Gorenstein, 1984; Gorenstein & Kar, 1975) suggested that the ^{31}P resonance of a phosphate diester in a g^-,g^- conformation (both P–O ester bonds have dihedral angles of −60° or −gauche, −*g*) should

†Supported by NIH (Grant AI27744), the Purdue University Biochemical Magnetic Resonance Laboratory, which is supported by NIH (Grant RR01077 from the Biotechnology Resources Program of the Division of Research Resources), the NSF National Biological Facilities Center on Biomolecular NMR, Structure and Design at Purdue (Grants BBS 8614177 and 8714258 from the Division of Biological Instrumentation), and the National AIDS Research Center at Purdue (Grant AI727713).

0006-2960/90/0429-5245$02.50/0

be several parts per million upfield of the ^{31}P signal of an ester in a g^-,t or t,t conformation (t, trans or 180° dihedral angle).

These initial theoretical calculations, and some more reliable gauge-invariant ^{31}P chemical shielding tensor calculations by Pullman and co-workers (Giessner-Prettre et al., 1984; Ribas-Prado et al., 1979) as well as some simple model studies (Gorenstein, 1981), suggested that we might be able to use this stereoelectronic effect on ^{31}P chemical shifts as a probe of nucleic acid conformations. Thus, as described above, if ^{31}P chemical shifts are sensitive to phosphate ester conformations, they potentially provide information on two of the most important torsional angles that define the nucleic acid deoxyribose phosphate backbone. One of these, the C3′–O3′–P–O5′ torsional angle (ζ), is also found to be the most variable one in the B-form of the double helix and the other, the O3′–P–O5′–C5′ torsional angle (α), is one of the most variable in the A-form of the duplex (Saenger, 1984). Indeed, following the original suggestion of Sundaralingam (1969) and on the basis of recent X-ray crystallographic studies of oligonucleotides, Saenger (1984) has noted that the P–O bonds may be considered the "major pivots affecting polynucleotide structure".

Variation of ^{31}P Chemical Shifts in Oligonucleotides. Earlier ^{31}P NMR studies on poly- and oligonucleic acids (Gorenstein et al., 1976; Gorenstein & Kar, 1975) supported the suggestion that the base-stacked, helical structure with a gauche, gauche phosphate ester torsional conformation should be upfield from the random coil conformation, which contains a mixture of phosphate esters in other nongauche conformations as well. More recently, we (Gorenstein et al., 1987a,b; Lai et al., 1984; Schroeder et al., 1986; Shah et al., 1984a) and others (Ott & Eckstein, 1985a,b; Petersheim et al., 1984; Ragg et al., 1989) have used a ^{17}O or $^{17}O/^{18}O$ labeling scheme or 2D heteronuclear correlation scheme (Fu et al., 1988; Gorenstein et al., 1988; Sklenar & Bax, 1987) to identify the individual ^{31}P resonances of oligonucleotides. These studies have allowed us to gain insight into the various factors responsible for ^{31}P chemical shift variations in oligonucleotides (Cheng et al., 1982, 1987; Ott & Eckstein, 1985b; Patel, 1974; Schroeder et al., 1986). As discussed above, one of the major contributing factors that we have hypothesized to determine ^{31}P chemical shifts is the main-chain torsional angles of the individual phosphodiester groups along the oligonucleotide double helix. Phosphates located toward the middle of a B-DNA double helix assume the lower energy, stereoelectronically (Gorenstein, 1987) favored g^-,g^- conformation, while phosphodiester linkages located toward the ends of the double helix tend to adopt a mixture of g^-,g^- and t,g^- conformations, where increased flexibility of the helix is more likely to occur. [The notation for the P–O ester torsion angles follows the convention of Seeman et al. (1976), with the ζ (P–O3′) angle given first, followed by the α (P–O5′) angle.] Because the g^-,g^- conformation is responsible for a more upfield ^{31}P chemical shift, while a t,g^- conformation is associated with a lower field chemical shift, internal phosphates in oligonucleotides would be expected to be upfield of those nearer the ends. Although several exceptions have been observed, this positional relationship appears to be generally valid for oligonucleotides where ^{31}P chemical shift assignments have been determined (Gorenstein, 1978; Gorenstein et al., 1976; Ott & Eckstein, 1985a,b; Schroeder et al., 1986, 1987). Thus position of the phosphorus (terminal versus internal) within the oligonucleotide is one important factor responsible for variations in ^{31}P chemical shifts. It should be noted that environmental effects on the ^{31}P chemical shifts of nucleic acids (Costello et al., 1976; Lerner & Kearns, 1980) are generally smaller than the intrinsic conformational factors discussed above, assuming comparisons are made under similar solvation conditions. Similarly, other possible effects, such as ring-current shifts, are not likely to be responsible for shifts >0.01 ppm (Giessner-Prettre et al., 1976; Gorenstein, 1984).

Eckstein and co-workers (Connolly & Eckstein, 1984; Ott & Eckstein, 1985a,b) and our laboratory (Gorenstein, 1987; Gorenstein et al., 1988) have recently noted that in addition to the "positional effect" there appears to be a sequence-specific effect on ^{31}P chemical shifts as well. As described in more detail below, local helical distortions arise along the DNA chain due to purine–purine steric clash on opposite strands of the double helix (Calladine, 1982; Dickerson, 1983). A modest correlation exists between the local helical parameters such as helix twist or roll and ^{31}P chemical shifts (Gorenstein et al., 1988; Ott & Eckstein, 1985a,b; Ragg et al., 1989).

Patel et al. (1982) have shown that the GT base-pair mismatch in the decamer duplex d(CGTGAATTCGCG)$_2$ provides some very interesting ^{31}P spectral shifts. Whereas the ^{31}P spectral dispersion is <0.7 ppm in normal B-DNA double helices, new signals are shifted upfield and downfield from the "normal" double-helical phosphate ^{31}P signals of the parent dodecamer duplex. Distortions in the normal Watson–Crick base-pairing structure are thus capable of perturbing the sugar phosphate backbone ^{31}P signals in a "site-specific" fashion.

In this paper we analyze the sequence-, position-, and site-specific variations in the ^{31}P chemical shifts and $J_{H3'-P}$ coupling constants of a number of base-pair mismatch duplexes. This has provided information on the backbone conformation of unusual DNA structures in solution. We demonstrate that there exists a good correlation between the backbone torsional angles ϵ and ζ and the ^{31}P chemical shifts.

Experimental Procedures

Synthesis and Sample Preparation. The self-complementary mismatch 12-mers d(CGTGAATTCGCG) (GT 12-mer), d(CGUGAATTCGCG) (GU 12-mer), d(CGGGAATTCGCG) (GG 12-mer), d(CGCGAATTCACG) (AC 12-mer), and d(CGAGAATTCGCG) (GA 12-mer) were synthesized by a manual modification of the phosphite triester method on a solid support as previously described (Lai et al., 1984; Schroeder et al., 1987; Shah et al., 1984b). The porous glass derivatized supports were synthesized as described (Gait, 1984).

Deoxyuridine 3′-Phosphoramidite Synthesis. 5′-*O*-(Dimethoxytrityl)deoxyuridine was synthesized as previously described (Schaller et al., 1963). The TLC indicated that the product was pure. The yield was 80%. 5′-*O*-(Dimethoxytrityl)deoxyuridine 3′-phosphoramidite was synthesized from 5′-*O*-(dimethoxytrityl)deoxyuridine following the procedure of Mcbribe and Caruthers (1983). The ^{31}P NMR of this sample gave one ^{31}P peak at −150 ppm referenced to H_3PO_4.

^{17}O Labeling. We have introduced the ^{17}O label into the phosphoryl group by replacing the I_2/H_2O in the oxidation step of the phosphite by $I_2/H_2{}^{17}O$ (Monsanto) as previously described (Lai et al., 1984; Shah et al., 1984b). After being cleaved from the suppport and deprotected, the resulting oligonucleotides were purified by reversed-phase HPLC (Schroeder et al., 1987) followed by dialysis.

^{31}P NMR samples generally contained 20–50 mg of purified oligomers in 0.4 mL of D_2O containing 25 mM Hepes, 10 nM EDTA, 75 mM KCl, and 0.1 mM NaN_3, pH* 8.0.

NMR. The ^{31}P NMR spectra were taken on a Varian

XL-200A (200 MHz ^1H) spectrometer at ambient temperature. The 1D ^{31}P NMR parameters for the 12-mers were as follows: sweep width 143 Hz; acquisition time 0.5 s; block size 512 zero-filled to 16K; pulse width 7.5 μs; spectra were resolution-enhanced with a combination of positive exponential and Gaussian apodization functions; the number of acquisitions was between 500 and 1000. ^{31}P NMR resonances are referenced to an external sample of trimethyl phosphate (TMP), which is 3.456 ppm downfield of 85% H_3PO_4. Assignments of the individual signals to the phosphates of the duplexes were accomplished by either site-specific ^{17}O labeling of the phosphoryl groups (Schroeder et al., 1987) or a combination of ^1H signal assignments from 2D $^1H/^1H$ NOESY and COSY followed by heteronuclear $^1H/^{31}P$ correlation PAC spectra (Fu et al., 1988; Gorenstein et al., 1988).

A $^{31}P/^1H$ *p*ure *a*bsorption *p*hase *c*onstant time (PAC) version of the Kessler–Griesinger long-range heteronuclear correlation (COLOC) experiment (Kessler et al., 1984) was conducted on the oligonucleotides (Fu et al., 1988; Jones et al., 1988). The PAC spectrum provides chemical shift correlation between the H3′, H4′, and H5′ protons of the deoxyribose rings and the three- or four-bond-coupled phosphorus. Coupling occurs between the phosphorus and the H3′ proton on the 5′ side and the H4′ and H5′ protons on the 3′ side of the dinucleotide fragment.

The PAC spectra were acquired with a sweep width of 122.8 Hz in the t_2 dimension and 641.9 Hz in the t_1 dimension. The experiments were collected with 400–600 transients for each of the 64 FIDs with 256 data points of resolution. A 90° pulse of 7.5 μs for phosphorus and 80 μs for protons was used. The data was processed with 1K zero filling in the t_1 dimension and 512 zero filling in the t_2 dimension. A Gaussian apodization was applied in both the t_1 and t_2 dimensions to give resolution enhancement.

Bax–Freeman Selective 2D J-Resolved Long-Range Correlation. This experiment with a Dante sequence for the selective 180° pulse (Sklenar & Bax, 1987) was performed on the duplexes to correlate the ^{31}P chemical shift with the H3′–phosphorus coupling constant. A Dante pulse chain consisted of 20 pulses of an approximate length of 9° (total of 180°). The selective 2D *J* data were acquired with a sweep width of 50 Hz in the t_1 dimension and 503.6 Hz in the t_2 dimension. A 90° phosphorus pulse width of 7.5 μs, an 8.8-μs proton pulse width, and a recycle delay of 1.5 s were used. The data set consisted of 1100–1600 transients for each of the 32 FIDs with 448 data points in t_1. The data were processed with 1K zero filling in both the t_2 and t_1 dimensions with a Gaussian apodization plus a negative exponential function to give resolution enhancement in both dimensions.

The observed three-bond coupling constants were analyzed with a proton–phosphorus Karplus relationship to measure the H3′–C3′–O–P torsional angle (θ), from which we have calculated the C4′–C3′–O–P torsional angle ($\epsilon = -\theta - 120°$). The relationship $J = 15.3 \cos^2\theta - 6.1 \cos\theta + 1.6$ was determined by Lankhorst et al. (1984).

The ^{31}P melting profiles of oligonucleotides were acquired over the temperature range of 20–80 °C in 5-deg increments. The 1D ^{31}P spectrum was referenced to an external sample of 85% phosphoric acid, which was recorded at each temperature interval. The temperatures of the ^1H-decoupled ^{31}P NMR samples were corrected for decoupler heating of the sample. The ^{31}P "thermometer" consisted of a sample of phosphoric acid and trimethyl phosphate as previously described (Gorenstein & Luxon, 1979). Note that even with WALTZ decoupling we find that decoupler heating can raise the temperature of the sample by as much as 4 °C.

Results

Assignment of ^{31}P Signals of Oligonucleotide Duplexes. The ^{31}P and PAC spectra for d(CGUGAATTCGCG) (GU 12-mer), d(CGGGAATTCGCG) (GG 12-mer), d(CGAGAATTCGCG) (GA 12-mer), and d(CGCGAATTCACG) (AC 12-mer) are shown in Figures 1 and 2, respectively. The ^{31}P spectra and assignments for other oligonucleotides discussed in this paper, including the self-complementary duplex 14-mers d(TGTGAGCGCTCACA), d(TATGAGCGCTCATA), d(TCTGAGCGCTCAGA), d(TGTGTGCGCACACA), d(TGTGACGCGTCACA), and d(CACAGTATACTGTG) (Gorenstein et al., 1988; Schroeder et al., 1987, 1989), the GT 12-mer d(CGTGAATTCGCG) (Gorenstein et al., 1988; Nikonowicz et al., 1989), and the 10-mer d(CCCGATCGGG) (Powers et al., 1989) have been previously reported. The ^{31}P signals were assigned by 2D pure absorption phase constant time (PAC) heteronuclear correlation NMR (Fu et al., 1988).

As shown in Figure 2, a representative PAC spectrum of the GU 12-mer contains a pair of cross-peaks between the phosphorus resonance and either an H3′/H4′ pair or an H3′/H5′ pair (other spectra not shown may be obtained from the authors upon request; Roongta, 1989). The proton signals have been previously assigned from the 2D $^1H/^1H$ NOESY and COSY spectra (V. A. Roongta et al., to be submitted; Roongta, 1989). These $^1H/^1H$ 2D spectra allow a complete sequence-specific assignment of all proton signals and confirm that all mismatches reported here are basically B-DNA duplexes. Assignment of the ^{31}P signal of the *i*th phosphate was achieved through connectivities with both the 3′H (*i*) and 4′H ($i + 1$) or 5′H ($i + 1$)/5″H ($i + 1$) deoxyribose protons (Lai et al., 1984; Pardi et al., 1983). Although the 5′H ($i + 1$) and 5″H ($i + 1$) protons overlap with the 4′ protons, the intensities for the ^{31}P–5′H and ^{31}P–5″H PAC cross-peaks generally appear to be much weaker than the 4′H cross-peaks. These pairs of protons from the PAC spectrum were then matched to appropriate pairs from the assigned ^1H spectrum to complete the assignment of the ^{31}P spectrum. The individual ^{31}P chemical shifts of the dodecamers are shown in Table I.

^{31}P Melting Curve. The melting transition of the oligonucleotide from the base-paired duplex structure to the unstacked random coil structure can be followed by ^{31}P chemical shifts, because the ^{31}P chemical shifts of the random coil DNA are downfield from duplex DNA (Gorenstein, 1981). This downfield shift is attributed to the change in conformation of the phosphate from a low-energy preferred g^-,g^- conformation of the ζ,α torsional angles in duplex DNA to various higher energy conformations (such as g^-,t and t,t) of the DNA in a random coil state. The ^{31}P melting curves for the GT, GG, GA, and GU 12-mers are shown in Figure 3. The GT and GU 12-mers show a sharp melting transition, while the GG and GA 12-mers show a very broad melting transition.

The 2D *J*-resolved spectrum at 18 °C for the GT 12-mer is shown in Figure 4. Additional *J*-resolved spectra at various temperatures are also shown in Figures 5 and 6 (*J*-resolved spectra for the other duplexes are comparable; spectra not shown). The coupling constants were measured from a slice taken in the t_1 dimension for each ^{31}P resonance in the 2D *J*-resolved spectra. We have utilized these coupling constants and a proton–phosphorus Karplus relationship (see Experimental Procedures) to determine the H3′–C3′–O–P torsional angle (θ), from which we have calculated the C4′–C3′–O–P torsional angle (ϵ). Up to four different torsional angles (0–360°) may be derived from the same coupling constant;

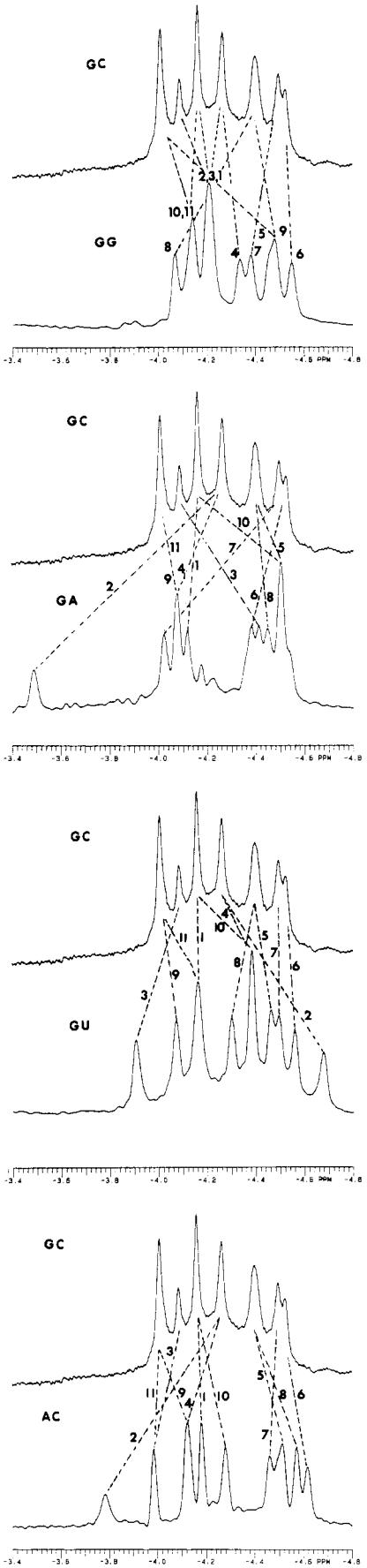

FIGURE 1: Comparison of the ^{31}P NMR spectra and phosphate assignments of the mismatch 12-mers with the base-paired GC 12-mer. Numbering corresponds to phosphate position from the 5′-end of the duplexes. (A) GG 12-mer. (B) GA 12-mer. (C) GU 12-mer. (D) AC 12-mer.

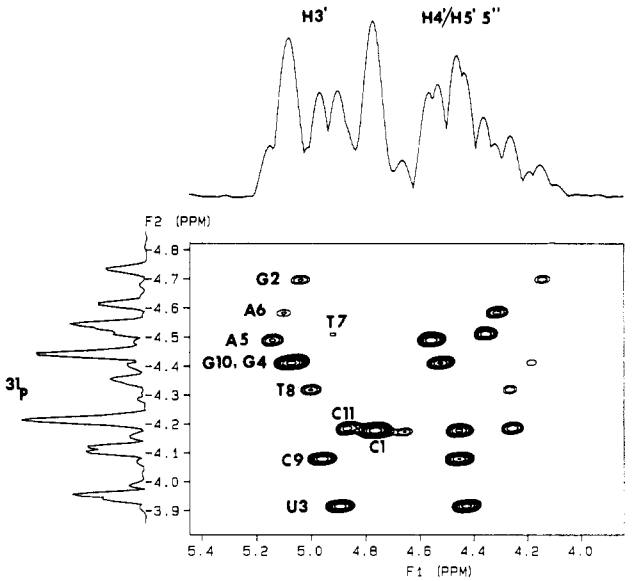

FIGURE 2: Two-dimensional $^{31}P/^{1}H$ PAC heteronuclear correlation NMR spectrum of the GU 12-mer mismatch duplex decamer at 200 MHz (^{1}H). The 1D decoupled ^{31}P NMR spectrum is shown along one axis, and the H3′, H4′, and H5′,5″ region of the proton spectrum is shown along the second axis.

we assume that the torsional angle closest to the crystallographically observed value of $\epsilon = -169° \pm 25°$ (Saenger, 1984) is the correct value. As shown by Dickerson's laboratory (Dickerson, 1983; Dickerson & Drew, 1981; Prive et al., 1988) and our laboratory (R. Powers et al., submitted), there is a strong correlation ($R = -0.92$) between torsional angles ζ and ϵ in the crystal structures of B-DNA duplexes [ζ may be calculated from the relationship $\zeta = -317 - 1.23\epsilon$ (Dickerson, 1983; Dickerson & Drew, 1981)]. Thus, assuming this correlation of ζ and ϵ exists for other duplex structures in solution as well, and from the measured $J_{H3'-P}$ coupling constants, we can calculate both C4′–C3′–O3′–P (ϵ) and C3′–O3′–P–O5′ (ζ) torsional angles. The experimentally measured $J_{H3'-P}$ coupling constants at different temperatures are listed for the GT, GG, GA, and GU 12-mer mismatches in Table II.

GT 12-mer. As previously reported [see Figure 3 in Gorenstein et al. (1988)], the ^{31}P signals of the G2 and T3 phosphates moved upfield and downfield, respectively, from those of the normal GC 12-mer. The phosphates in the middle, i.e., A5, A6, and T7, show very little variation from the parent GC 12-mer. The other phosphorus resonances do show small shifts, and these perturbations from the shifts of the parent 12-mer are more pronounced near the mismatch. From the ^{31}P melting curve (Figure 3A) of the GT 12-mer, the T3 phosphate moves upfield with increase in temperature, which is in the opposite direction from the downfield shifts of all the other phosphates.

The 2D *J*-resolved spectrum of the GT 12-mer at 18 °C is shown in Figure 4. There is some error in the measurement of the coupling constants for A5, G10, and G4 residues due to significant overlap of the ^{31}P resonances.

The 2D *J*-resolved spectrum of the GT 12-mer at 50 °C is shown in Figure 5. The plot of variation of the coupling constants with temperature is shown in Figure 7. It is interesting to note that the Py-Pu type of base steps show less variation in coupling constant with temperature than the other types of base steps. Generally the coupling constants increase with temperature. At 80 °C the coupling constant is nearly the same for all of the ^{31}P resonances of all mismatch oligonucleotides (cf. Figure 6). Significantly, the variations with temperature in the ^{31}P chemical shifts and in the coupling

Table I: ^{31}P Chemical Shifts[a] of the Five Mismatches at Ambient Temperature

GT 12-mer[b]	^{31}P shifts	GG 12-mer[c]	^{31}P shifts	GA 12-mer[c]	^{31}P shifts	GU 12-mer[c]	^{31}P shifts	AC 12-mer[c]	^{31}P shifts
C1	-4.078	C1	-4.198	C1	-4.140	C1	-4.177	C1	-4.211
G2	-4.670	G2	-4.198	G2	-3.493	G2	-4.713	G2	-3.783
T3	-3.897	*G3*	-4.198	*A3*	-4.292	*U3*	-3.909	*C3*	-4.003
G4	-4.371	G4	-4.345	G4	-4.140	G4	-4.420	G4	-4.159
A5	-4.408	A5	-4.462	A5	-4.571	A5	-4.494	A5	-4.561
A6	-4.523	A6	-4.548	A6	-4.246	A6	-4.691	A6	-4.665
T7	-4.463	T7	-4.375	T7	-4.005	T7	-4.518	T7	-4.509
T8	-4.247	T8	-4.044	T8	-4.444	T8	-4.323	T8	-4.656
C9	-4.047	C9	-4.486	C9	-4.069	C9	-4.079	C9	-4.146
G10	-4.386	*G10*	-4.132	*G10*	-4.521	*G10*	-4.420	*A10*	-4.327
C11	-4.154	C11	-4.132	C11	-4.150	C11	-4.177	C11	-4.003
G12		G12		G12		G12		G12	

[a] ^{31}P chemical shifts are referenced to TMP (trimethyl phosphate) at room temperature. [b] The ^{31}P resonances of the GT 12-mer were assigned by site-specifically labeling each phosphate with ^{17}O (Gorenstein et al., 1988). [c] The ^{31}P resonances of all the other mismatches were assigned by using the $^{31}P/^{1}H$ HETCOR (PAC) 2D experiment.

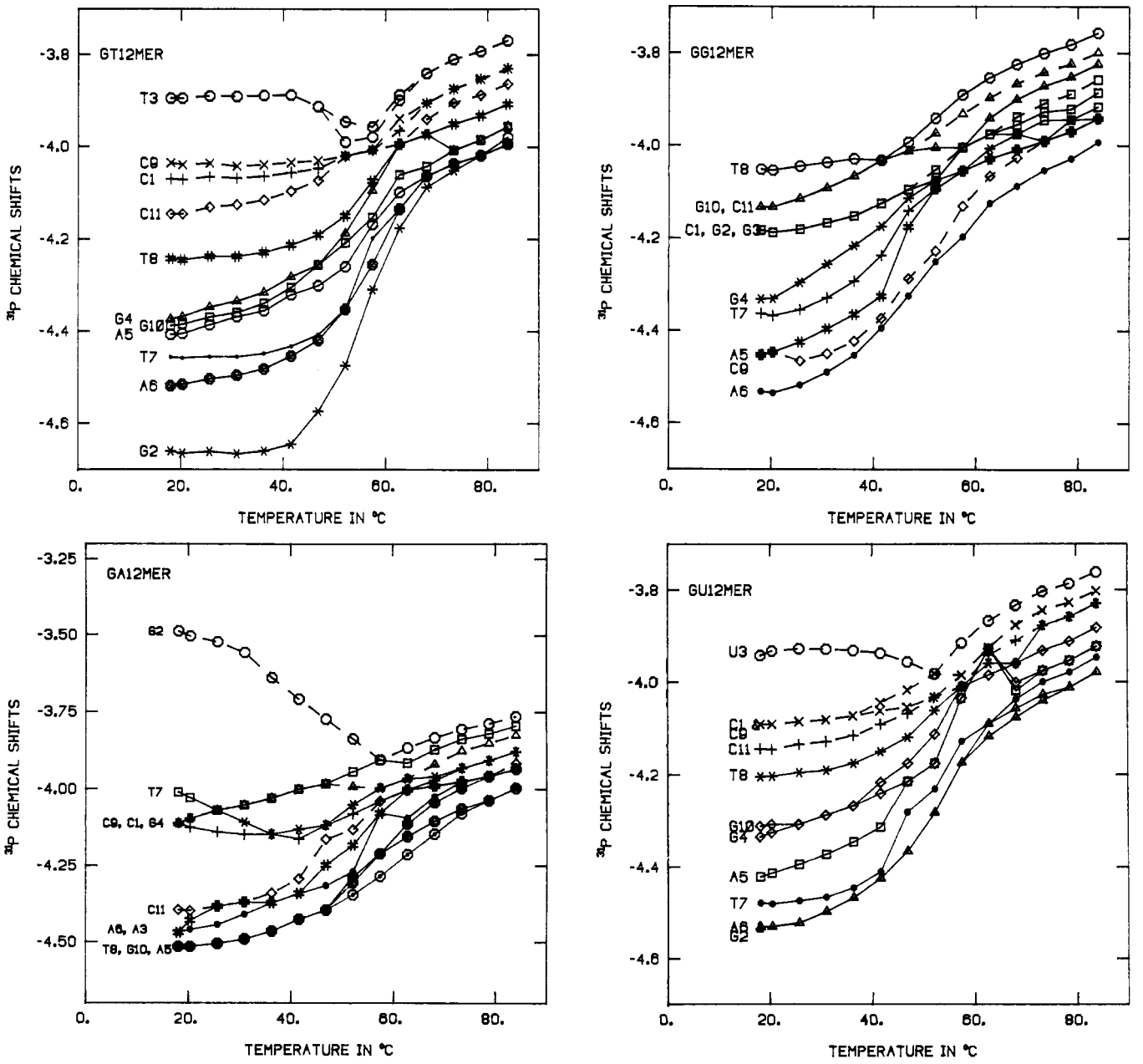

FIGURE 3: Temperature dependence of ^{31}P chemical shifts of duplex mismatches. Because of overlap of the signals in the melting region (40–50 °C), the signals at higher temperature are only tentatively assigned. (A) GT 12-mer. (B) GG 12-mer. (C) GA 12-mer. (D) GU 12-mer.

constants for each of the phosphates follow parallel behavior (compare Figure 7 with Figure 3A). The effective melting temperature, as measured from either the coupling constant or ^{31}P chemical shift melting plots, is the same ($T_m \sim 50$–60 °C). The temperature dependence to the $J_{H3'-P}$ coupling constant of C9, however, appears unusual. Because of overlap and poor resolution for the small coupling constants (especially at lower temperatures), the errors in the measurements may

Table II: $J_{H3'-P}$ Coupling Constants at 18, 30, 50, and 80 °C for the GT, GG, GA, and GU 12-mers[a]

	GT 12-mer				GG 12-mer				GA 12-mer				GU 12-mer			
nucleotide	18 °C	30 °C	50 °C	80 °C	18 °C	30 °C	50 °C	80 °C	18 °C	30 °C	50 °C	80 °C	18 °C	30 °C	50 °C	80 °C
1Cp	5.5	7.2	5.7	6.7	5.4	5.8	7.2	7.2	5.9	5.7	6.3	7.3	5.3	5.9	6.4	6.5
2Gp	2.6	und	2.1	6.6	5.4	5.8	5.1	6.3	8.7	7.9	6.4	7.1	und	und	3.2	6.2
3Cp, Tp, Up, Gp, or Ap	6.2	6.5	5.7	6.9	5.4	5.8	5.1	6.3	und	und	4.6	6.4	5.9	5.8	6.4	7.0
4Gp	3.1	2.7	3.7	6.8	2.0	und	5.1	6.5	5.9	6.3	6.3	7.3	1.8	2.3	4.8	6.7
5Ap	3.1	3.5	2.1	6.6	und	und	5.3	6.5	und	und	4.0	6.0	und	und	4.7	6.7
6Ap	1.3	1.5	3.6	6.6	2.5	1.8	5.1	7.2	und	und	5.1	6.4	und	und	3.2	6.2
7Tp	2.2	und	3.6	6.6	und	3.7	5.2	6.5	6.2	5.7	6.7	6.6	und	und	3.9	6.7
8Tp	1.5	und	3.3	6.2	6.0	5.4	6.5	7.0	und	und	4.3	6.4	2.8	3.8	6.0	7.0
9Cp	4.3	7.2	5.7	6.7	und	und	5.1	6.5	5.9	5.7	5.7	7.1	4.9	5.9	6.0	6.5
10Gp or Ap	3.1	3.5	3.5	6.8	5.9	5.9	5.5	6.7	und	und	4.3	6.90	1.8	2.3	5.2	7.0
11Cp	5.5	6.3	6.2	6.8	5.9	5.9	5.8	7.0	und	und	6.2	6.4	5.3	6.2	6.4	7.0

[a] und: the coupling constants were not determined because the multiplets were not resolved. Estimated error is ±0.2 Hz.

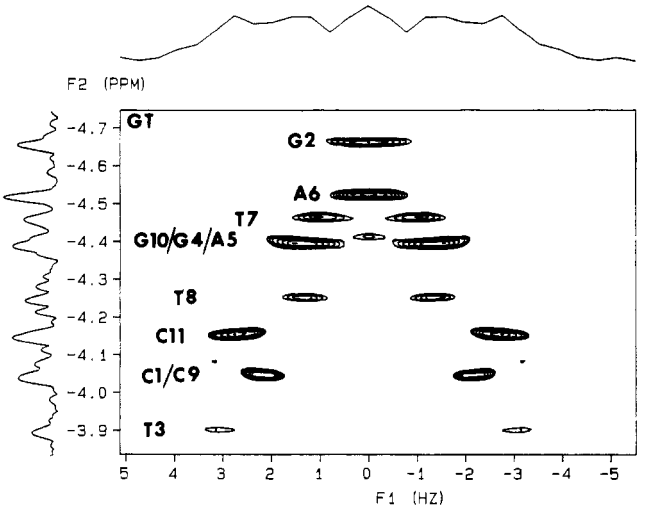

FIGURE 4: 2D *J*-resolved $^{31}P/^{1}H$ spectrum of the GT 12-mer duplex decamer at 18 °C. The 1D decoupled ^{31}P NMR spectrum is also shown along one axis, and the H3′ coupled doublets are shown along the second dimension.

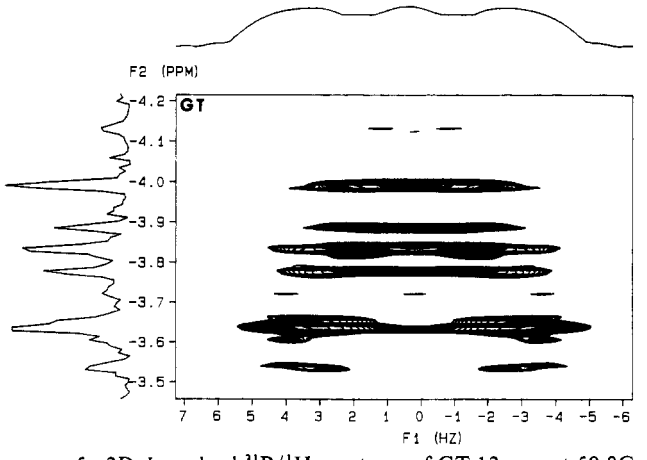

FIGURE 5: 2D *J*-resolved $^{31}P/^{1}H$ spectrum of GT 12-mer at 50 °C. The 1D projections of the ^{31}P spectra along the *t*2 dimension and the H3′ coupled doublet along the *t*1 dimension are also plotted.

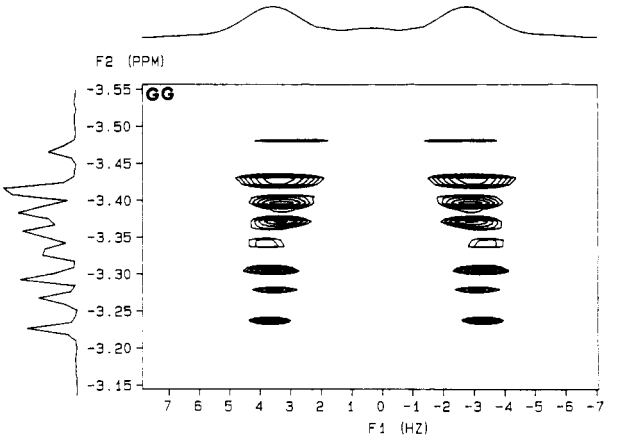

FIGURE 6: 2D *J*-resolved $^{31}P/^{1}H$ spectrum of GG 12-mer at 80 °C. The 1D projections of the ^{31}P spectra along the *t*2 dimension and the H3′ coupled doublet along the *t*1 dimension are also plotted.

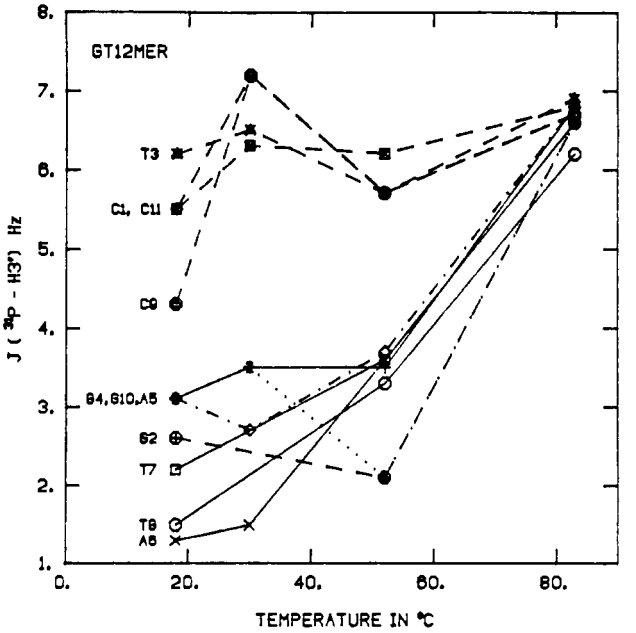

FIGURE 7: A plot of variation of the $J_{H3'-P}$ coupling constant with temperature for the GT 12-mer. The dashed curve denotes the Py-Pu base steps, and the solid curve denotes the Pu-Py and nonclashing base steps.

be as large as ±0.5–1 Hz for some of the phosphates. In general, the phosphates that show less variation in ^{31}P chemical shift with temperature are the same ones that show less variation in the coupling constant with temperature.

In Figure 9A the variations in calculated torsional angles (based upon the measured $J_{H3'-P}$ coupling constants), ^{31}P chemical shifts, and predicted helix twist are plotted against the sequence. ^{31}P chemical shifts and the torsional angles show similar sequence-specific trends. In addition, the phosphates at the ends correlate well with the predicted helix twist. Both the ^{31}P chemical shifts and the calculated torsional angles follow the positional relationship in the middle of the sequence.

GG 12-mer. Surprisingly, all phosphorus resonances of the GG 12-mer fall in a narrow region. There is a great deal of overlap in the ^{31}P spectrum (and in addition there is an underlying hump beneath the resonances). The PAC 2D spec-

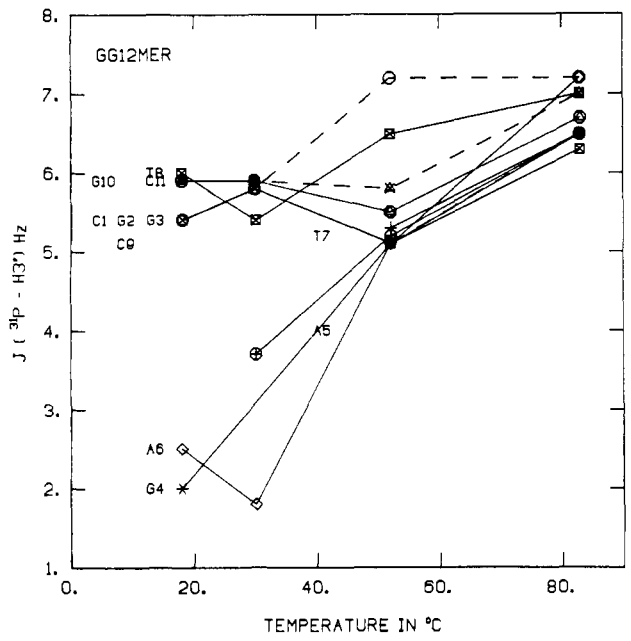

FIGURE 8: A plot of variation of the $J_{H3'-P}$ coupling constant with temperature for the GG 12-mer duplex. The dashed curve denotes the Py-Pu base steps, and the solid curve denotes the Pu-Py and nonclashing base steps.

trum (Figure 2A) also shows some overlap. The assignments of the GG 12-mer are compared to those of the parent GC 12-mer in Figure 1A. The T8 phosphate is the most downfield resonance, which is rather surprising because it is two base pairs removed from the mismatch site. The C9 phosphate signal has moved upfield when compared to the C9 of the GT and GC 12-mers. The ^{31}P melting curve of the GG 12-mer (Figure 3B) shows a very broad melting transition.

As seen from Table II, only some of the $J_{H3'-P}$ coupling constants were resolved for this mismatch. The coupling constant of the T8 resonance in the GG 12-mer is larger than that observed in any of the other mismatches, and at the same time the T8 phosphate in this mismatch is the most downfield T8 resonance of any of the mismatches. This is surprising because it is two base pairs removed from the actual site of the mismatch. This observation suggests that the GG mismatch at position 3 is responsible for major distortions in the backbone structure.

The $J_{H3'-P}$ coupling constants were well resolved when the 2D J-resolved $^1H/^{31}P$ spectra were collected at higher temperatures (cf. Figure 6). Again, the variation in the coupling constants with temperature (Figure 8) is similar to the variation in ^{31}P chemical shifts with temperature (see also Figure 3B).

The variations of the calculated torsional angles, ^{31}P shifts, and predicted helix twist are shown in Figure 9B. The ^{31}P shifts and the torsional angles follow parallel trends, but as expected because of the nature of the mismatch, there is no correlation of chemical shifts with predicted helix twist.

GA 12-mer. The ^{31}P spectrum of the GA 12-mer is quite different from that of the GC 12-mer (Figure 1B). The ^{31}P spectrum of this mismatch is comparable to the unassigned 1D spectrum reported by Patel et al. (1984a). The assignments of the A3 and A6 phosphates are interchangeable due to the lack of H3'-P cross-peaks for these phosphates (at least partially attributable to the small $J_{H3'-P}$ coupling constants to these residues). The ^{31}P melting curve (Figure 3B) shows that the downfield G2 phosphate resonance shifts dramatically upfield with an increase in temperature in a premelting transition. At the melting transition the G2 phosphate signal shifts downfield with increase in temperature as do all the other phosphates. The melting transitions for all of the phosphates are broad as compared with the GT or the GU 12-mer. This downfield shift of the G2 phosphate resonance suggests that the phosphate is in a higher energy, more trans P–O ester conformation at low temperature. As the temperature is increased, the backbone becomes more flexible and the G2 phosphate can now adopt the normal low-energy state (more gauchelike P–O ester conformation). This downfield shift of G2 in the GA 12-mer is directly opposite to the upfield shift of G2 in the GT 12-mer at room temperature.

Only a few $J_{H3'-P}$ coupling constants could be measured at lower temperature for the GA 12-mer, although the coupling constants at 50 and 80 °C were well resolved. The G2 phosphate has the largest coupling constant (8–8.5 Hz), which as expected is also the most downfield of the ^{31}P signals. The changes in the coupling constants with temperature (Table II; plot not shown) follow a pattern similar to that observed for the changes in ^{31}P chemical shifts with temperature (Figure 3C). It is important to note that the coupling constant for the G2 phosphate first decreases and then increases again with temperature, which is exactly the same behavior seen for its chemical shift.

GU 12-mer. The 1D spectrum of the GU 12-mer (Figure 1C) is essentially the same as that of the GT 12-mer. The G2 phosphate signal moves upfield and the U3 moves downfield relative to the GC 12-mer signals (Figure 1C), again identical with the shifts of the G2 and T3 phosphates in the GT 12-mer. It should be noted that the ^{31}P spectrum appears to be dependent upon the concentration of the DNA sample and also upon the ionic strength (Roongta, 1989). The ^{31}P melting curve and the 2D J-resolved spectrum of the GU 12-mer (Figure 3D) are also quite similar to those of the GT 12-mer (Figure 3A).

The measured coupling constants from the 30, 50, and 80 °C 2D J-resolved spectra (spectra not shown) are listed in Table II. The temperature dependence to the coupling constants (spectra not shown) and ^{31}P chemical shifts (Figure 3D) parallel each other and are quite similar to the plots for the GT 12-mer.

In Figure 9D the variations of ^{31}P chemical shifts, $J_{H3'-P}$ coupling constants, and predicted helical twist are plotted against the sequence. Overall the ^{31}P shifts and the torsional angles follow similar trends.

AC 12-mer. The ^{31}P NMR spectrum of the AC 12-mer is comparable to that reported by Patel et al. (1984b), and the resonances were assigned from the 2D PAC spectra (Figure 2D). The G2 phosphate resonance shifts downfield and the T8 phosphate resonance shifts upfield relative to the GC 12-mer. All of the other ^{31}P resonances behave similarly to those of the GT 12-mer.

Discussion

Site-, Position-, and Sequence-Specific Variation of ^{31}P Chemical Shifts and Backbone Torsional Angles of Base-Pair Mismatch 12-mers. Patel et al. (1982) had earlier shown that base-pair mismatch in a duplex (GT 12-mer) provided some very interesting site-specific ^{31}P spectral shifts. Our laboratory has utilized both ^{17}O labeling and 2D heteronuclear correlation experiments to assign the phosphate signals for this GT mismatch (Gorenstein et al., 1988). Whereas the ^{31}P spectral dispersion is <0.7 ppm in normal B-DNA double helices, new signals are shifted upfield and downfield from the "normal" double-helical phosphate ^{31}P signals of the parent GC 12-mer, $d(CGCGAATTCGCG)_2$. A comparison of the ^{31}P resonance assignments for the Dickerson base-paired GC 12-mer [as-

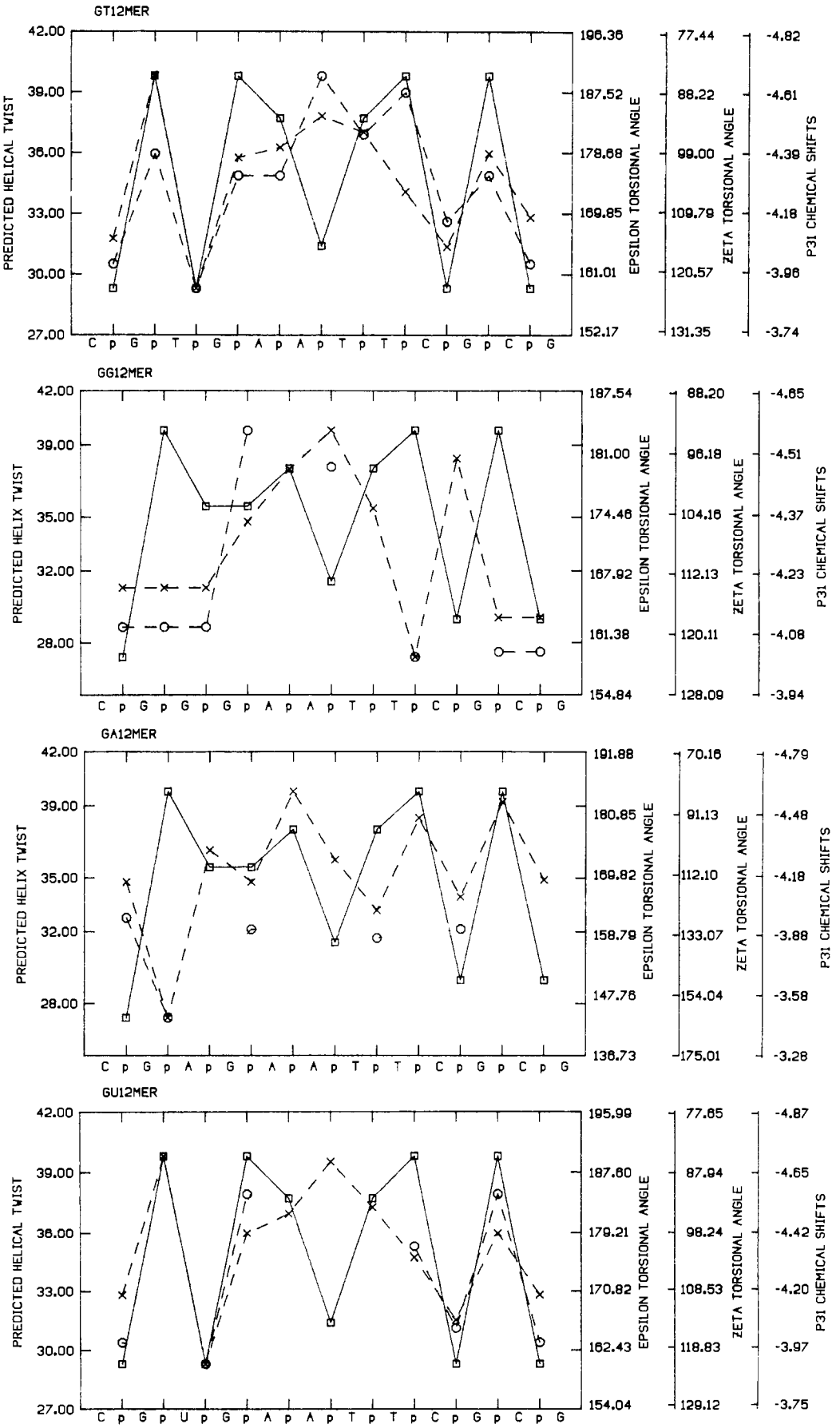

FIGURE 9: Comparison of ^{31}P chemical shifts (--×--), P–O3′ ester torsional angle $|\zeta|$ and C–O3′ torsional angle $|\epsilon|$ (--○--), and predicted helix twist based upon the Calladine rules (–□–) versus position for the duplex 12-mers. (A) GT 12-mer. (B) GG 12-mer. (C) GA 12-mer. (D) GU 12-mer. The ζ torsional angle was calculated from the $J_{H3'-P}$ coupling constants derived from Figure 4, the ϵ torsional angle was calculated from the Karplus relationship, and the correlation between ϵ and ζ is $\zeta = -317 - 1.23\epsilon$. The helix twist, t_g, is derived from the calculated helix twist $\sum_1$ sum function and $t_g = 35.6 + 2.1\sum_1$.

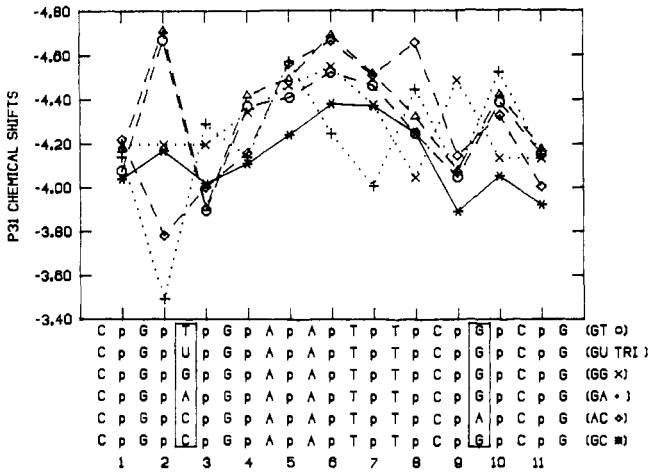

FIGURE 10: Summary comparison of the ^{31}P chemical shifts of the mismatches and the GC 12-mer versus position along the 5′–3′ strand for the mismatches duplexes. The GT 12-mer (○), GU 12-mer (△), and AC 12-mer (◇) are shown by dotted lines (···). The GG 12-mer (×) and GA 12-mer (+) are shown by the dashed lines (- - -). The GC 12-mer (*) is shown by the solid line.

signments are from Ott and Eckstein (1985a)] and the mismatch 12-mers GG, GA, GU, and AC is shown in Figure 1. A summary of the ^{31}P chemical shifts versus sequence for all of the mismatches is shown in Figure 10.

It is clear that phosphate position 2 (numbering from the 5′-end) is the one most perturbed by the mismatch at the third residue. It is interesting to note that for both the GT and the GU 12-mers the G2 phosphate resonance shifts upfield and the phosphate 3 signal shifts downfield. The variations in ^{31}P chemical shifts for the rest of the GT and GU 12-mer phosphates are similar to the GC 12-mer ^{31}P chemical shift variations. The G2 phosphate resonance of the AC 12-mer shifts downfield, which is in the opposite direction from that seen for G2 of the GT and GU 12-mers. The T8 phosphate signal of the AC 12-mer shifts upfield, which is surprising because it is two base pairs removed from the mismatch site. The variations of the ^{31}P shifts for the other AC 12-mer phosphates are similar to those of the GC 12-mer and the purine–pyrimidine mismatches. The ^{31}P spectrum of the GG 12-mer has considerable overlap. It is surprising to note that there are no "anomalous" ^{31}P resonances shifted outside of the main cluster of peaks in the GG 12-mer when compared to other mismatches. The G2 and G3 phosphates do not show any large perturbation from their normal ^{31}P shifts in the parent GC 12-mer. Only the C9 phosphate resonance moves upfield, which is opposite from all the other sequences. The rest of the ^{31}P chemical shifts follow the same trend as the GC, GT, and GU 12-mers. The ^{31}P spectrum of the GA 12-mer also has considerable overlap. The G2 phosphate signal is considerably shifted to low field. The T7 resonance of the GA 12-mer has also shifted downfield when compared to other mismatches. The rest of the ^{31}P resonances follow the same trend as for all the other mismatches.

The dispersion in the ^{31}P chemical shifts in the oligonucleotides is related to the structure, sequence, and position of the phosphate in the oligonucleotide (Connolly & Eckstein, 1984; Gorenstein, 1981; Gorenstein et al., 1988; Ott & Eckstein, 1985a). In addition to these mismatch "site-specific" structural effects on the ^{31}P chemical shifts, as mentioned above, another factor that will also affect ^{31}P chemical shifts is the degree of conformational constraint imposed by the duplex geometry. Our laboratory has suggested that two of the most important parameters controlling ^{31}P chemical shifts in phosphate esters are the P–O torsional angles [in nucleic acids the P–O5′ (α) and P–O3′ (ζ) torsional angles (Gorenstein, 1987; Gorenstein & Kar, 1975)] and the C–O5′ (β) and C–O3′ (ϵ) torsional angles (Giessner-Prettre et al., 1984; Ribas-Prado et al., 1979), although the P–O torsional angle may be more important. Note that the ^{31}P chemical shift of phosphates (Figure 10) moves upfield the more interior the phosphate. Base pairs closer to the ends of the duplex are less constrained to the stacked, base-paired geometry. This "fraying" at the ends imparts greater conformational flexibility to the deoxyribose phosphate backbone, and thus phosphates at the ends of the duplex will tend to adopt more of a mixture of g^-,g^- and t,g^- conformations. Interior phosphates are more constrained to the polymer P–O g^-,g^- conformation (Connolly & Eckstein, 1984; Gorenstein, 1981, 1987; Ott & Eckstein, 1985a,b). One thing in common for all mismatches is the upfield shift of the ^{31}P resonances as we move to the middle of the sequence and away from the mismatch, consistent with this positional effect.

These position- and site-specific ^{31}P chemical shift effects are apparently superimposed on a sequence-specific effect as well (Connolly & Eckstein, 1984; Gorenstein et al., 1988; Ott & Eckstein, 1985a,b; Ragg et al., 1989; Schroeder et al., 1986, 1987). In the B-form DNA double helix with ~10 base pairs per turn (360°) of the helix, each base pair is rotated ca. +36° (helix twist) with respect to the nearest-neighbor base pair. However, analysis (Dickerson, 1983) of X-ray crystallographic structures of a number of duplexes has revealed large variations in local helix structure, with helix twist varying from 25 to 45°. Although a set of "Calladine rules" has been defined for these variations (Calladine, 1982), more recent crystallographic studies of additional B-DNA structures have suggested that these sequence-specific variations are more complex (Prive et al., 1988). However, correlations between experimentally measured P–O and C–O torsional angles and results from molecular mechanics/dynamics energy minimization calculations show that these results are consistent with the hypothesis that sequence-specific variations in ^{31}P chemical shifts are at least partially attributable to sequence-specific changes in the deoxyribose phosphate backbone (Gorenstein et al., 1988; R. Powers et al., submitted). The ^{31}P chemical shifts of duplex B-DNA phosphates correlate reasonably well with some aspects of the original Dickerson/Calladine calculated values for variation in the helical twist (or base-pair roll) of the individual base steps in the oligonucleotides.

The variations of the ^{31}P chemical shifts and the predicted helical twist (see legend, Figure 9) against sequence are shown for all mismatches in Figures 9 and 10. As seen from these figures, the GC, GT, and GU 12-mer chemical shifts give a good correlation with the predicted helical twist. The correlation is about 0.7. The GG, GA, and AC 12-mer chemical shifts do not correlate well with the predicted helical twist. The high correlation of the GT and GU 12-mers was surprising, but at the same time these mismatches, which retain a Pu-Py base pair, likely distort the duplex geometry less than a Pu-Pu base-pair mismatch.

$J_{H3'-P}$ Coupling Constants from 2D $^1H/^{31}P$ J-Resolved Spectra. These site-, position-, and sequence-specific effects have been attributed to variations in the phosphate ester backbone torsional angles (Gorenstein, 1981; Gorenstein & Kar, 1975; Gorenstein et al., 1988; Ott & Eckstein, 1985a). Using the selective 2D *J*-resolved long-range correlation pulse sequence, we can measure the three-bond H3′–C3′–O–P coupling constants (Figure 4; listed in Table II) for each of the phosphates of the duplex oligonucleotides (Gorenstein et al., 1988; Sklenar & Bax, 1987). In combination with a

proton–phosphorus Karplus relationship (see Experimental Procedures), we can determine the H3′–C3′–O–P torsional angle (θ), from which we have calculated the C4′–C3′–O–P (ϵ) and C3′–O–P–O5′ (ζ) torsional angles (see Results). Plots of the variation of ζ, ^{31}P chemical shifts, and calculated helix twist versus position for the decamer sequences are shown in Figure 9. As shown in Figure 4, generally the ^{31}P signals of phosphates at Pu-Pu, Pu-Py, and Py-Py base steps are upfield and have smaller $J_{H3'-P}$ coupling constants. The phosphates of Py-Pu base steps have downfield ^{31}P signals and larger coupling constants.

From the 2D J spectra for 12 different oligonucleotide duplexes, we have observed that in general the $J_{H3'-P}$ coupling constants for the upfield-shifted signals are invariably smaller than those of the downfield signals. This results in a characteristic 2D J spectrum where the coupling constant monotonically decreases from low to high field (Figures 4–6). It is difficult to resolve the very smallest $J_{H3'-P}$ coupling constants (<2 Hz) for the upfield ^{31}P resonances. The consistency of the overall pattern to the various 2D J-resolved spectra (cf. Figure 4) implies that the $J_{H3'-P}$ coupling constants (and the derived ζ or ϵ torsional angles) are strongly correlated with the ^{31}P chemical shifts (Gorenstein et al., 1988, 1990a; Ragg et al., 1989). A plot of ζ or ϵ vs ^{31}P chemical shifts for various duplex 10-, 12-, 13-, and 14-mers at 18 °C is shown in Figure 11 (correlation coefficient R = −0.81). The correlation coefficient between ζ (or ϵ) and ^{31}P chemical shifts is also quite good at different temperatures; R = −0.79 (at ambient temperature), −0.77 (at 50 °C), and even −0.70 (at 80 °C) (plots not shown).

The deviations from the best-fit straight line can be due to peak overlap, resulting in over- or underestimation of the coupling constants, or to additional factors contributing to ^{31}P chemical shift variations. However, the important point from the correlation is that upfield ^{31}P resonances have small coupling constants and downfield ^{31}P resonances have large coupling constants. Importantly, the conformational distortions due to the mismatches are accommodated in this relationship, for example, the G2 phosphate of the GA 12-mer. This G2 shows an abnormally large coupling constant but still lies very close to the best straight line. This observation strongly supports our hypothesis that ^{31}P chemical shifts are very much dependent upon the backbone conformation of oligonucleotides.

Origin of ^{31}P Chemical Shift Variations. The origin of the site-, position-, and sequence-specific effects on ^{31}P chemical shifts can thus be understood in terms of perturbations in the deoxyribose phosphate backbone conformation. Changes in the deoxyribose phosphate backbone can occur at one or all of the angles α–ζ:

$$P^{\alpha}–O5'^{\beta}–C5'^{\gamma}–C4'^{\delta}–C3'^{\epsilon}–O3'^{\zeta}–P$$

Thus, structural perturbations in the duplex arising from base-pair mismatch will alter the local helical parameters (such as helical twist or base-pair roll). Changes in these local parameters will generally alter the length of the deoxyribose phosphate backbone (Gorenstein et al., 1988)—thus winding or unwinding the helix requires stretching or contracting the deoxyribose phosphate backbone between the two stacked base pairs. To a significant extent, these changes in the overall length of the deoxyribose phosphate backbone "tether" are reflected in changes in the P–O ester (as well as other) torsional angles.

The variations in the P–O (and C–O) torsional angles as the result of changes in the length of the backbone tether may provide the linkage between the site-specific, position-specific, and Calladine-rule-type sequence-specific structural variations

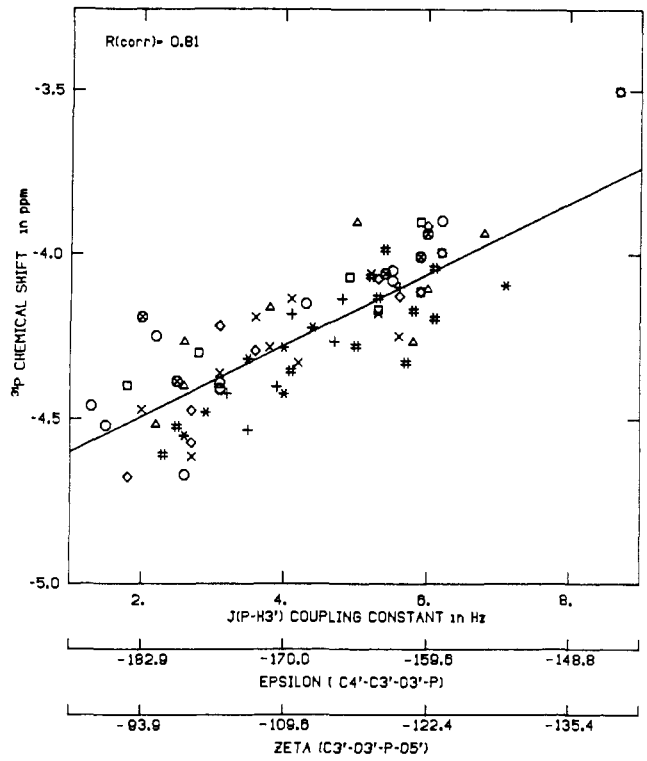

FIGURE 11: Correlation of ^{31}P chemical shifts (18 °C) with experimentally determined $J_{H3'-P}$ coupling constants (18 °C, first X-axis) and calculated ϵ (second X-axis) and ζ (third X-axis) torsional angles. The data include GT 12-mer (○), GU 12-mer (□), GA 12-mer (□ superimposed on ◇), GG 12-mer (⊗), 10-mer d(CCCGATCGGG)$_2$ (△), and 14-mers d(TATGAGCGCTCATA)$_2$ (+), d(TGTGTGCGCACACA)$_2$ (×), d(TGTGACGCGTCACA)$_2$ (#), d(TGTGAGCGCTCACA)$_2$ (◇), and d(CACAGTATACTGTG)$_2$ (*). Assignment of the GC 12-mer is from Ott and Eckstein (1985a), and $J_{H3'-P}$ coupling constants of the GC 12-mer were from Sklenar and Bax (1987). The $J_{H3'-P}$ coupling constants and assignments of the 14-mers and the GT 12-mer are from Gorenstein et al. (1988), Schroeder et al. (1986), and Schroeder et al. (1989), and those of the 10-mer are from Powers et al. (1989).

in the duplex and ^{31}P chemical shifts. Analysis of the X-ray crystal structure (Dickerson, 1983; Dickerson & Drew, 1981; Saenger, 1984) of the B-form GC 12-mer has shown that torsional angles α, β, and γ on the 5′-side of the sugar are largely constrained to values g^- (−60°), t (180°), and g (+60°), whereas significant variations are observed on the 3′-side of the deoxyribose phosphate backbone. The greatest variation in backbone torsional angles is observed for ζ (P–O3′) followed by ϵ (C3′–O3′). It is important to note that ϵ and ζ torsional angle variations are highly correlated in B-DNA, with a correlation coefficient of −0.92 (Dickerson, 1983; Dickerson & Drew, 1981; Saenger, 1984; R. Powers et al., submitted). In addition, α and γ torsional angle variations are also highly correlated in A-DNA, with a correlation coefficient also of −0.92 (Shakked & Rabinovitch, 1986) (β is constrained to a trans conformation in both B- and A-DNA). As noted by Dickerson (Dickerson, 1983; Dickerson & Drew, 1981), when the P–O3′ (ζ) conformation is g^-, invariably the C–O3′ conformation (ϵ) is found to be t. This ϵ (t), ζ (g^-) conformation is the most common backbone conformation [defined as the B_I (t,g) conformation (Dickerson, 1983; Dickerson & Drew, 1981)]. The other most common conformation for the ϵ,ζ pair is the g^-,t or B_{II} state. [Similar A_I and A_{II} conformations may be defined for the A-DNA conformational state; see Shakked and Rabinovitch (1986).] A "crankshaft" motion interconverts B_I and B_{II} (or A_I and A_{II}) conformations with only a modest movement of the phosphate. It is largely this variation in ϵ

and ζ [as well as δ (Dickerson, 1983; Dickerson & Drew, 1981; Gorenstein et al., 1988)] that allows the sugar phosphate backbone to "stretch" or "contract" to allow for variations in the local structure of B-DNA.

Thus these conformational changes may provide an explanation for much of the observed variation in ^{31}P chemical shifts and coupling constants. As mentioned above, two of the most important parameters controlling ^{31}P chemical shifts in phosphate esters are the P–O torsional angles (in nucleic acids the α and ζ torsional angles) (Gorenstein, 1987; Gorenstein & Kar, 1975) and C–O torsional angles (β and ϵ) (Giessner-Prettre et al., 1984; Ribas-Prado et al., 1979), although the P-O torsional angle may be more important. It is thus most significant that, by using the measured $J_{H3'-P}$ coupling constants from the 2D J-resolved spectra, there appears to be a strong correlation between $J_{H3'-P}$ coupling constants and ^{31}P chemical shifts (R = ca. −0.8). The data of Figure 11 strongly support our hypothesis that the site-, position-, and sequence-specific variations in ^{31}P chemical shifts are largely attributable to perturbations in the local geometry and the backbone torsional angles (at least for ζ and ϵ).

B_I/B_{II} Populations. In Dickerson's correlation (Dickerson, 1983; Dickerson & Drew, 1981) between ϵ and ζ torsional angles, most phosphates were in the B_I or B_{II} conformational states (with B_I predominating). The B_I conformation represents the low-energy phosphate state (t,g^-) and the B_{II} conformation represents the high-energy phosphate state (g^-,t). A few phosphate conformations in the crystal state of the B-DNA GC 12-mer also clustered along the line connecting the B_I and B_{II} end points in the ϵ vs ζ plot, suggesting that intermediate states were also possible. However, the B_I and B_{II} states represent ground-state minima with the P–O and C–O torsional angles in the staggered conformations (Gorenstein et al., 1977; Kollman et al., 1982). Partially or fully eclipsed conformations that are not energy minima are only accessible through libration in each of the staggered states or through transient passage during the rapid jumps between the two ground states. Thus it may be possible to analyze the variation in the $J_{H3'-P}$ coupling constants in terms of fractional populations of the two thermodynamically stable B_I and B_{II} states. [Note: X-ray studies have also shown that the other staggered ϵ torsional angle of g^+ is not accessible (Saenger, 1984).] For our correlation purposes, we have used the average values of the ϵ and ζ torsional angles for these two states as calculated from the crystal structure data. The average ϵ torsional angle value for the B_I state is −190° and for the B_{II} state is −105° (Dickerson, 1983; Dickerson & Drew, 1981). These ϵ values approximate the maximum possible range of $J_{H3'-P}$ coupling constants (for ϵ = −105°, $J_{H3'-P}$ = 10.0 Hz, and for ϵ = −190°, $J_{H3'-P}$ = 1.3 Hz). In addition, in this torsional angle range the Karplus curve is nearly a single-valued function (actually it is only single-valued in the range of $\epsilon \sim$ −200 to −120°; between −105 and −120°, the coupling constant is in the range of 10.0–10.8 Hz). The measured coupling constant represents the weighted average of the coupling constants in the two states, and by using the two extreme values of ϵ, we have estimated the percentage in the B_I state from the relationship

$$\%\ B_I = 100\% - \%\ B_{II} \sim \frac{J_{H3'-P}(\text{obsd}) - J_{H3'-P}(-105°)}{J_{H3'-P}(-190°) - J_{H3'-P}(-105°)} \times 100 \quad (1)$$

Under these assumptions and from the plot of Figure 11, we can estimate that the ^{31}P chemical shift and $J_{H3'-P}$ coupling constant of a phosphate in a purely B_I conformational state should be ca. −4.6 ppm and 1.3 Hz, respectively. Similarly, the ^{31}P chemical shift and $J_{H3'-P}$ coupling constant of a phosphate in a purely B_{II} conformational state should be ca. −3.0 ppm and 10 Hz, respectively. The ^{31}P chemical shift difference between the B_I and B_{II} conformational states is thus estimated to be 1.6 ppm. We have previously calculated that the ^{31}P chemical shift of a B_{II}-type phosphate ($\zeta = t$) is ca. 1.5 ppm downfield of a phosphate in a B_I conformation ($\zeta = g^-$) (Gorenstein, 1981, 1984; Gorenstein & Kar, 1975). It is thus extremely gratifying that these results fully support our hypothesis on the conformational dependence to ^{31}P chemical shifts. The largest coupling constant that we measure is ca. 7–8 Hz, which represents a ζ angle of about −120°. Analysis of the coupling constants in terms of the fractional populations of the B_I and B_{II} states show that phosphates with $J_{H3'-P}$ near this maximum value have nearly equal populations of the B_I and B_{II} states. At 80 °C, based upon the observed coupling constants, the B_I and B_{II} states are also about equally populated in the random coil single-strand form of the oligonucleotides. This is quite reasonable because on the basis of molecular orbital calculations we have previously estimated that the B_I phosphate ester conformation is less than 1.0 kcal/mol lower energy than the B_{II} conformation (Gorenstein, 1987; Gorenstein et al., 1977).

From this analysis we suggest that the dispersion in the ^{31}P chemical shifts of oligonucleotides is largely attributable to different ratios of populations of the B_I and B_{II} states for each phosphate in the sequence. Assuming that only the staggered rotamers define stable conformations, the phosphate is assumed to make rapid jumps between the two states. Alternatively, the phosphate could be considered to be constrained to a single intermediate P–O ester conformation. This later explanation appears to be ruled out by restrained molecular dynamics simulations (R. Powers and D. G. Gorenstein, submitted), which clearly show that these intermediate conformational states are only transiently populated as the phosphate makes rapid crankshaft transitions between the B_I and B_{II} states. Thus the measured coupling constant appears to indeed reflect the populations of these two possible conformational states. Significantly, the NOESY-distance-restrained molecular dynamics calculations (R. Powers and D. G. Gorenstein, submitted) reproduce quite accurately the measured sequence-specific variation in the $J_{H3'-P}$ coupling constants (in these calculations no torsional angle restraints are placed on the phosphate ester backbone).

Temperature Dependence to ^{31}P Chemical Shifts and Coupling Constants. The correlation between ϵ (or ζ) and ^{31}P chemical shifts is strengthened further by the temperature dependence of both ^{31}P chemical shifts and $J_{H3'-P}$ coupling constants. As shown in Figure 3, the ^{31}P chemical shift of each phosphate not directly adjacent to the mismatch sites in the 12-mers [as well as all of the other base-paired oligonucleotides—data not shown; see also Gorenstein et al. (1988, 1990a,b), Ragg et al. (1989), and Schroeder et al. (1989)] shifts downfield with increasing temperature. The $J_{H3'-P}$ coupling constant of the phosphates also increases with increasing temperature except for some of those phosphates near mismatch sites.

At 80 °C, above the melting temperature of the duplexes, there is very little variation in the coupling constants, and the dispersion in the ^{31}P chemical shifts is also very small for all of the oligonucleotides. The resolution in the J dimension of the 2D J-resolved spectra is much better at the higher temperatures due to the increase in the transverse relaxation times

of the phosphates. The coupling constants at 80 °C vary between 5.5 and 7 Hz, with most of the data points near 6.5 Hz, and ^{31}P chemical shifts are dispersed over a much narrower spectral range (<0.2 ppm). This translates into average ϵ of −160° and ζ of −122°. The large and uniform coupling constants and small dispersion in ^{31}P chemical shifts at high temperature are reflective of a random coil conformation for the melted duplexes.

Sequence-Specific Effects on ϵ and ζ Torsional Angles. As shown in Figure 9 the ^{31}P chemical shifts of the GT and GU mismatches generally follow sequence-specific effects [see also Gorenstein et al. (1988) and Schroeder et al. (1989)]. Thus these Pu-Py base-pair mismatches appear not to greatly distort the phosphate ester conformations in the immediate region around the mismatch, while the GG and GA mismatches follow no regular sequence-specific variation, as might be expected because of the unusual nature of these mismatch sites. In general, ^{31}P chemical shifts of Py-Pu base steps are downfield from those of Pu-Py, Pu-Pu, and Py-Py base steps (Gorenstein et al., 1988; Ott & Eckstein, 1985a; Schroeder et al., 1989). Due to the clash in the minor groove, Py-Pu base steps produce the greatest unwinding of the helix.

Site- and Position-Specific Effects. The unusual downfield-shifted ^{31}P signals in the mismatch 12-mers and an extrahelical adenosine 13-mer (Nikonowicz et al., 1989) are all associated with a large $J_{H3'-P}$, consistent with our hypothesis that the phosphate ester conformation is largely responsible for these ^{31}P chemical shift perturbations. In particular, in the GT and GU 12-mers the most downfield signal is associated with the phosphate on the 3′-side of the mismatch (phosphate 3 on the 5′-strand) while the most upfield signal is associated with the phosphate on the 5′-side of the mismatch (phosphate 2 on the 5′-strand). Similar, although less extreme, perturbations in the ^{31}P chemical shifts are observed for the corresponding phosphates on the opposite 3′-strand. A more complex pattern emerges for the GG, GA, and AC mismatches. Thus in the GG mismatch phosphate 8 on the 5′-strand is the most downfield signal. In the GA and AC mismatchs the phosphate on the 5′-side of the mismatch (phosphate 2) is the most downfield signal. As in extrahelical base duplexes (Nikonowicz et al., 1989; Roy et al., 1987), there is no uniform pattern for the direction or magnitude of the ^{31}P chemical shift perturbation, other than that they generally represent phosphates proximate to the site of duplex distortion. However, in *every* instance the perturbation in the ^{31}P chemical shifts is directly reflected by a parallel perturbation in the $J_{H3'-P}$ coupling constants (Figure 9), thus demonstrating that these complex ^{31}P chemical shifts changes directly reflect different adjustments in the sugar phosphate backbone to the nature of the mismatch.

Superimposed on these sequence- and site-specific effects is a positional effect. The position-specific effect is based upon the observation that in many duplexes the more interior the phosphate, the more upfield the ^{31}P chemical shift. In keeping with the correlation between ^{31}P chemical shifts and $J_{H3'-P}$, the interior phosphates that obey the positional effect have more upfield ^{31}P chemical shifts *and* smaller $J_{H3'-P}$ coupling constants. The conformations of these interior phosphates are thus nearly 100% in the B_I state. We do not entirely understand at this time why certain sequences show good correlations with the sequence-specific variations in helix twist predicted by Calladine rules and ^{31}P chemical shifts/$J_{H3'-P}$ coupling constants (ϵ and ζ) while other sequences show excellent correlations between position and ^{31}P chemical shifts and $J_{H3'-P}$ coupling constants. As indicated above, this could also reflect the current concern over the validity of the Calladine rules in general. Certainly one important variable is the presence or absence of a base step with a minor groove clash (a Py-Pu base step). Thus the GC 12-mer sequence (where the central six residues have no minor groove clash) shows a good correlation ($R = -0.81$) between position of the phosphate from the ends of the duplex and ϵ and ζ torsional angles. If the pure B_I state can be ascribed to a polymerlike conformation, then the ^{31}P data suggest that the more interior phosphates are more polymerlike and that, even in a 12-mer, end effects are evident even at the fifth and sixth phosphates. Thus "fraying", or at least increased conformational freedom, appears from analysis of the backbone conformations to extend much further into the interior of oligonucleotide duplexes than previously appreciated.

Also as shown in Figures 9 and 10, with the exception of the site-specific shifted phosphates at the second and third positions on both strands (numbering from the 5′-end), the phosphates at the 3′-end of the strand are more polymerlike (higher population of the B_I state) than the phosphates at the equivalent position but on the 5′-end of the strand. It is quite interesting that the conformation of the ith phosphate from the 5′-end of the strand (○) is nearly exactly equivalent to the conformation of the $(i + 1)$th phosphate from the 3′-end of the strand (△). This asymmetry has been previously noted in the ^{31}P chemical shifts as well (Gorenstein et al., 1988).

It is to be emphasized that the correlation between ^{31}P chemical shifts and $J_{H3'-P}$ coupling constants is *always* valid despite the complexities of the position-, site-, and sequence-specific variations.

Conclusions

In general, the ^{31}P chemical shifts and coupling constants of those phosphates in the five mismatch 12-mers furthest from the mixmatch sites are quite similar to those of the GC 12-mer. The signal shifted the most either upfield or downfield occurs at phosphate position 2 adjacent to the site of mismatch. Perturbations at other sites are more complex. The effect of a GT or GU base-pair mismatch on ^{31}P chemical shifts and $J_{H3'-P}$ coupling constants is largely localized to the base pairs adjacent to the site of mismatch. In contrast, the AC, GA, and GG mismatches create major distortions in the backbone structure, and the distortion is still felt several base pairs away. It has previously been reported that the local geometry in the GA mismatch is not distorted much beyond the mismatch itself (Patel et al., 1984b). This suggests that the effect of the mismatch is felt more in the backbone than the actual base pairing.

We have shown that there is a substantial correlation between ^{31}P chemical shifts and the experimentally measured C–O (ϵ) and the derived P–O (ζ) torsional angles. The data of Figures 7–10 support our hypothesis that the position-, site-, and sequence-specific effects on ^{31}P chemical shifts are largely attributable to variations in the helical parameters and the backbone torsional angles (at least for ζ and ϵ). Unwinding or winding the double helix changes the backbone torsional angles, and these backbone changes presumably are responsible for the variations in the ^{31}P chemical shifts of oligonucleotides [see Powers and Gorenstein (submitted)]. It is especially gratifying that the unusual downfield-shifted signals correlate well with the large $J_{H3'-P}$ and hence large ζ torsional angle. Apparently these base-pair mismatches distort the phosphodiester backbone. This alteration in the length of the phosphodiester tether is presumably accomplished by the phosphate switching from the normal B-DNA conformation (B_I) in which both P–O torsional angles ζ and α are in the g^- conformation

($\epsilon = t$) to a B_{II}-like conformation ($\epsilon = g^-$, $\zeta = t$, $\alpha = g^-$). The ^{31}P signal of a phosphate in a B_{II} conformation has now been confirmed by the $J_{H3'-P}$ coupling constant analysis to be $\sim$1.5–1.8 ppm downfield from the g^-,g^- phosphate in the B_I conformation, as originally predicted (Gorenstein, 1981).

These results provide strong support to our hypothesis that site-, position-, and sequence-specific variations in ^{31}P chemical shifts are attributable to these backbone-linked changes in duplex geometry. Major variations in the local helical structure (e.g., helix twist and roll angle) as well as other duplex distortions resulting from base-pair mismatch and extrahelical base inserts also appear to be reflected in perturbations in the deoxyribose phosphate ester backbone torsional angles. ^{31}P NMR spectroscopy therefore appears to be able to provide a powerful probe of these structural variations along the backbone of the DNA in solution.

ACKNOWLEDGMENTS

We greatly appreciate the contributions of Robert Powers.

REFERENCES

Assa-Munt, N., & Kearns, D. R. (1984) *Biochemistry 23*, 791.
Broido, M. A., Zon, G., & James, T. L. (1984) *Biochem. Biophys. Res. Commun. 119*, 663–670.
Calladine, C. R. (1982) *J. Mol. Biol. 161*, 343–352.
Cheng, D. M., Kan, L.-S., Miller, P. S., Leutzinger, E. E., & Ts'o, P. O. P. (1982) *Biopolymers 21*, 697.
Cheng, D. M., Kan, L., & Ts'o, P. O. P. (1987) *Phosphorus NMR in Biology* (Burt, C. T., Ed.) pp 135–147, CRC Press, Inc., Boca Raton, FL.
Clore, G. M., Gronenborn, A. M., Brunger, A. T., & Karplus, M. (1985) *J. Mol. Biol. 186*, 435–455.
Connolly, B. A., & Eckstein, F. (1984) *Biochemistry 23*, 5523–5527.
Costello, A. J. R., Glonek, T., & Van Wazer, J. R. (1976) *Inorg. Chem. 15*, 972–974.
Dickerson, R. E. (1983) *J. Mol. Biol. 166*, 419–441.
Dickerson, R. E., & Drew, H. R. (1981) *J. Mol. Biol. 149*, 761–786.
Feigon, J., Leupin, W., Denny, W. A., & Kearns, D. R. (1983) *Biochemistry 22*, 5930–5942, 5943–5951.
Frechet, D., Cheng, D. M., Kan, L.-S., & Ts'o, P. O. P. (1983) *Biochemistry 22*, 5194–5200.
Fu, J. M., Schroeder, S. A., Jones, C. R., Santini, R., & Gorenstein, D. G. (1988) *J. Magn. Reson. 77*, 577–582.
Gait, M. J. (1984) *Oligonucleotide Synthesis: A Practical Approach*, IRL press, Oxford, England.
Giessner-Prettre, C., Pullman, C., Borer, B., Kan, L.-S., & Ts'o, P. O. P. (1976) *Biopolymers 15*, 2277.
Giessner-Prettre, C., Pullman, B., Ribas-Prado, F., Cheng, D. M., Iuorno, V., & Ts'o, P. O. P. (1984) *Biopolymers 23*, 377.
Gorenstein, D. G. (1978) in *Jerusalem Symposium, NMR in Molecular Biology* (Pullman, B., Ed.) pp 1–15, D. Reidel Publishing Co., Dordrecht, The Netherlands.
Gorenstein, D. G. (1981) *Annu. Rev. Biophys. Bioeng. 10*, 355.
Gorenstein, D. G. (1983) *Prog. NMR Spectrosc. 16*, 1–98.
Gorenstein, D. G. (1984) in *Phosphorus-31 NMR: Principles and Applications* (Gorenstein, D. G., Ed.) Academic Press, New York.
Gorenstein, D. G. (1987) *Chem. Rev. 87*, 1047–1077.
Gorenstein, D. G., & Kar, D. (1975) *Biochem. Biophys. Res. Commun. 65*, 1073–1080.
Gorenstein, D. G., & Luxon, B. A. (1979) *Biochemistry 18*, 3796–3804.
Gorenstein, D. G., Findlay, J. B., Momii, R. K., Luxon, B. A., & Kar, D. (1976) *Biochemistry 15*, 3796–3803.
Gorenstein, D. G., Luxon, B. A., & Findlay, J. B. (1977) *Biochim. Biophys. Acta 475*, 184–190.
Gorenstein, D. G., Schroeder, S., Miyasaki, M., Fu, J., Jones, C., Roongta, V., & Abuaf, P. (1987a) *Proc. Int. Conf. Phosphorus Chem., 10th 30*, 567–570.
Gorenstein, D. G., Schroeder, S. A., Miyasaki, M., Fu, J. M., Roongta, V., Abuaf, P., Chang, A., & Yang, J. C. (1987b) *Biophosphates and Their Analogues—Synthesis, Structure, Metabolism and Activity* (Bruzik, K. S., & Stec, W. J., Eds.) pp 487–502, Elsevier Press, Amsterdam, The Netherlands.
Gorenstein, D. G., Schroeder, S. A., Fu, J. M., Metz, J. T., Roongta, V. A., & Jones, C. R. (1988) *Biochemistry 27*, 7223–7237.
Gorenstein, D. G., Jones, C. R., Schroeder, S. A., Metz, J. T., Fu, J. M., Roongta, V. A., Powers, R., & Karslake, C. (1990a) *Progress in Inorganic Biochemistry and Biophysics* (Gray, H., & Bertini, I., Eds.), Birkhauser, Inc., Boston (in press).
Gorenstein, D. G., Meadows, R. P., Metz, J. T., Nikonowicz, E., & Post, C. P. (1990b) in *Advances in Biophysical Chemistry* (Bush, C. A., Ed.) JAI Press, Greenwich, CT (in press).
Hare, D. R., Wemmer, D. E., Chou, S. H., Drobny, G., & Reid, B. (1983) *J. Mol. Biol. 171*, 319.
Hochschild, A., & Ptashne, M. (1986) *Cell 44*, 681.
James, T. L. (1984) in *Phosphorus-31 NMR: Principles and Applications* (Gorenstein, D. G., Ed.) pp 349–400, Academic Press, Orlando, FL.
Jones, C. R., Schroeder, S. A., & Gorenstein, D. G. (1988) *J. Magn. Reson. 80*, 370–374.
Kearns, D. R. (1984) *Crit. Rev. Biochem. 15*, 237–290.
Kessler, H., Griesinger, C., Zarbock, J., & Loosli, H. R. (1984) *J. Magn. Reson. 57*, 331–336.
Kollman, P., Keepers, J. W., & Weiner, P. (1982) *Biopolymers 21*, 2345.
Lai, K., Shah, D. O., Derose, E., & Gorenstein, D. G. (1984) *Biochem. Biophys. Res. Commun. 121*, 1021.
Lankhorst, P. P., Haasnoot, C. A. G., Erkelens, C., & Altona, C. (1984) *J. Biomol. Struct. Dyn. 1*, 1387–1405.
Lerner, D. B., & Kearns, D. R. (1980) *J. Am. Chem. Soc. 102*, 7612–7613.
Martin, K., & Schleif, R. F. (1986) *Proc. Natl. Acad. Sci. U.S.A. 83*, 3654.
Mcbribe, L. J., & Caruthers, M. H. (1983) *Tetrahedron Lett. 24*, 245.
McClarin, J. A., Frederick, C. A., Wang, B. C., Greene, P., Boyer, H. W., Grable, J., & Rosenberg, J. M. (1986) *Science 234*, 1526–1541.
Nikonowicz, E., Roongta, V., Jones, C. R., & Gorenstein, D. G. (1989) *Biochemistry 28*, 8714–8725.
Nilges, M., Clore, G. M., Gronenborn, A. M., Brunger, A. T., Karplus, M., & Nilsson, L. (1987) *Biochemistry 26*, 3718–3733.
Ott, J., & Eckstein, F. (1985a) *Biochemistry 24*, 253.
Ott, J., & Eckstein, F. (1985b) *Nucleic Acids Res. 13*, 6317–6330.
Pardi, A., Walker, R., Rapoport, H., Wider, G., & Wüthrich, K. (1983) *J. Am. Chem. Soc. 105*, 1652.
Patel, D. J. (1974) *Biochemistry 13*, 2396–2402.
Patel, D. J., Kozlowski, S. A., Marky, L. A., Broka, C., Rice, J. A., Itakura, K., & Breslauer, K. J. (1982) *Biochemistry 21*, 428–436.
Patel, D. J., Kozlowski, S. A., Ikuta, S., & Itakura, K. (1984a) *Biochemistry 23*, 3207.

Patel, D. J., Kozlowski, S. A., Ikuta, S., & Itakura, K. (1984b) *Biochemistry 23*, 3218.
Patel, D. J., Shapiro, L., & Hare, D. (1987) *Biophys. Chem. 16*, 423-454.
Petersheim, M., Mehdi, S., & Gerlt, J. A. (1984) *J. Am. Chem. Soc. 106*, 439-440.
Powers, R., Olsen, R. K., & Gorenstein, D. G. (1989) *J. Biomol. Struct. Dyn. 7*, 515-556.
Prive, G. G., Heinemann, U., Chandrasegaran, S., Kan, L. S., Kopka, M. L., & Dickerson, R. E. (1988) *Structure and Expression* (Sarma, R. H., & Sarma, M. H., Eds.) Vol. 2, Adenine Press, Guilderland, NY.
Ragg, E., Mondelli, R., Garbesi, A., Colonna, F. P., Battistini, C., & Vioglio, S. (1989) *Magn. Reson. Chem. 27*, 640-646.
Ribas-Prado, F., Giessner-Prettre, C., Pullman, B., & Daudey, J.-P. (1979) *J. Am. Chem. Soc. 101*, 1737.
Rinkel, L. J., van der Marel, G. A., van Boom, J. H., & Altona, C. (1987) *Eur. J. Biochem. 163*, 275-286.
Roontga, V. A. (1989) Ph.D. Thesis, Purdue University, West Lafayette, IN.
Roy, S., Sklenar, V., Appella, E., & Cohen, J. S. (1987) *Biopolymers 26*, 2041-2052.
Saenger, W. (1984) *Principles of Nucleic Acid Structure*, Springer-Verlag, New York.
Schaller, H., Weinmann, G., Lerch, B., & Khorana, H. G. (1963) *J. Am. Chem. Soc. 85*, 3821.
Scheek, R. M., Boelens, R., Russo, N., van Boom, J. H., & Kaptein, R. (1984) *Biochemistry 23*, 1371-1376.
Schroeder, S., Jones, C., Fu, J., & Gorenstein, D. G. (1986) *Bull. Magn. Reson. 8*, 137-146.
Schroeder, S., Fu, J., Jones, C., & Gorenstein, D. G. (1987) *Biochemistry 26*, 3812-3821.
Schroeder, S. A., Roongta, V., Fu, J. M., Jones, C. R., & Gorenstein, D. G. (1989) *Biochemistry 28*, 8292-8303.
Seeman, N. C., Rosenberg, J. M., Suddath, F. L., Park Kim, J. J., & Rich, A. (1976) *J. Mol. Biol. 104*, 142-143.
Shah, D. O., Lai, K., & Gorenstein, D. G. (1984a) *Biochemistry 23*, 6717-6723.
Shah, D. O., Lai, K., & Gorenstein, D. G. (1984b) *J. Am. Chem. Soc. 106*, 4302.
Shakked, Z., & Rabinovitch, D. (1986) *Prog. Biophys. Mol. Biol. 47*, 159-195.
Sklenar, V., & Bax, A. (1987) *J. Am. Chem. Soc. 109*, 7525-7526.
Sundaralingam, M. (1969) *Biopolymers 7*, 821-860.
van de Ven, J. M., & Hilbers, C. W. (1988) *Eur. J. Biochem. 178*, 1-38.

Lysine-329 of Murine Leukemia Virus Reverse Transcriptase: Possible Involvement in the Template-Primer Binding Function†

Venkata B. Nanduri and Mukund J. Modak*
Department of Biochemistry and Molecular Biology, New Jersey Medical School and Graduate School of Biomedical Sciences, University of Medicine and Dentistry of New Jersey, Newark, New Jersey 07103
Received October 5, 1989; Revised Manuscript Received January 31, 1990

ABSTRACT: Treatment of murine leukemia virus reverse transcriptase (MuLV RT) with 4-(oxoacetyl)-phenoxyacetic acid (OAPA) results in the loss of DNA polymerase as well as template-primer binding activity but has no effect on the RT-associated RNase-H activity. Binding stoichiometry revealed that approximately 3 mol of OAPA bound per mole of enzyme, when complete enzyme activation occurred. However, in the presence of template-primer, OAPA does not abolish polymerase activity and 2 mol of OAPA remains bound to 1 mol of enzyme. This observation suggests that only one OAPA reactive site is responsible for the loss of polymerase activity. This site was located on a single tryptic peptide by comparing the maps of the native enzyme and the enzyme treated with OAPA in the presence and absence of template-primer. The appearance of a new peptide peak eluting at 125 min from a C-18 reverse-phase column was consistently noted in the tryptic digest of enzyme treated with OAPA. This peak was absent in tryptic peptides made from the control enzyme or the enzyme protein that was treated with OAPA in the presence of activated DNA or synthetic template-primers. Amino acid composition and sequence analyses of this peptide revealed that it spanned residues 312-342 in the primary amino acid sequence of MuLV RT. Since this peptide does not contain arginine residues and Lys-329 exhibited resistance to tryptic digestion, we conclude that Lys-329 is the target of OAPA action. The correlation of the loss of enzyme activity with modification of Lys-329 by OAPA with concomitant loss of template-primer binding activity strongly implicates Lys-329 in the template-primer binding function of MuLV RT.

Moloney murine leukemia virus reverse transcriptase (MuLV RT)[1] is a single polypeptide enzyme, with a molecular mass of approximately 80 000 daltons, which expresses both polymerase and RNase-H activities (Dickson et al., 1982). The complete amino acid sequence of MuLV RT has been deduced from the nucleotide sequence of a noninfectious proviral DNA (Shinnick et al., 1981) and the exact location

† Supported in part by a grant from the New Jersey Commission on Cancer Research (CCR-86-487).
* Address correspondence to this author at Dept. of Biochemistry and Molecular Biology, UMDNJ—New Jersey Medical School, 185 South Orange Ave., Newark, NJ 07103-2714.

[1] Abbreviations: MuLV, Moloney murine leukemia virus; RT, reverse transcriptase; PLP, pyridoxal 5'-phosphate; TPCK, L-1-(tosylamido)-2-phenylethyl chloromethyl ketone; HPLC, high-performance liquid chromatography; TCA, trichloroacetic acid; TFA, trifluoroacetic acid; DTT, dithiothreitol; BSA, bovine serum albumin; Hepes, 4-(2-hydroxyethyl)-1-piperazineethanesulfonic acid; TP, template-primer; OAPA, 4-(oxoacetyl)phenoxyacetic acid; HIV, human immunodeficiency virus; BLV, bovine leukemia virus; RSV, Rous sarcoma virus; HTLV, human T-cell leukemia virus; act. DNA, activated deoxyribonucleic acid.

0006-2960/90/0429-5258$02.50/0